CHAPTER IV

RESULTS AND DISCUSSION

This chapter shows how to construct the optimal network for rainfall-runoff relationship. It is based on the selection of the suitable range [a, b] of linear transformation determined by statistical evaluation of the experimental results. For model development, the total input-target of 2,403 patterns are used for (1) training set consisting of 1,443 input-target patterns, and (2) testing set consisting of 960 input-target patterns. The feedforward backpropagation network is composed of one input layer, one output layer, and two hidden layers. The type of neurons connection in the network is fully connected. To implement the neural network toolbox, the sigmoid function, characterized by "*logsig*", is used as the activation function in both hidden and output layers. The backpropagation network training function (BTF, in (3.6)) is based on the Levenberg-Marquardt training function characterized by "*trainlm*" as the weight modification approach. The performance function is mean square error characterized by "*mse*". The network is generated by a function *newff* (3.6) as follows:

$$net = newff(PR,[N_{H_1}, N_{H_2}, 1],\{'logsig','logsig','logsig'\},'trainlm','mse'),$$

where N_{H_1} and N_{H_2} are the number of neurons in the first and second hidden layers, respectively.

In the training process, the initial parameters for specifying the maximum values of training cycles and the goal of minimizing mean square error are set as follows:

$net.trainParam.epochs = 2000,$ and

$net.trainParam.goal = 0.00005.$

The number of neurons in each hidden layer is varied from 12 neurons to 30 neurons in this study. To find the optimal network, four ranges of transformation

[a, b] are examined. There are [0.3, 0.7], [0.2, 0.8], [0.1, 0.9] and [0.05, 0.95] denoted by L1,L2,L3 and L4, respectively. In addition, the two cases of model input are used with the network *net*. For the first case (I1), the input vector composes of three lags of rainfall and discharges as given in (3.2), this is expressed as

$$\mathrm{I1}(t_i) = [R(t_i - 6)\ R(t_i - 5)\ R(t_i - 4)\ D(t_i - 3t_D)\ D(t_i - 2t_D)\ D(t_i - t_D)]^T .$$

For the second case (I2), the input vector is similar as case I1 with the inclusion of the last 24 hours of discharge from the predicted time ($D(t_i - 24)$). It is given by

$$\mathrm{I2}(t_i) = [R(t-6)\ R(t_i - 5)\ R(t_i - 4)\ D(t_i - 3t_D)\ D(t_i - 2t_D)\ D(t_i - t_D)\, D(t_i - 24)]^T . \quad (4.1)$$

The optimal network structure depends on the variation of the range of transformation $\{\mathrm{Li}\}_{i=1}^{4}$ and the two cases of model input are obtained by trial and error procedure based on the average absolute relative error. The number of hidden layers (N_{H_i}) is varied between 12 to 30 neurons. For the specified network structure, it is trained with ten distinctive sets of initial weights and biases used in the training process and validated with the testing set. The output of the trained network is rescaled by (3.12) in order to compare with the corresponding target. Experimental results of the optimal network structures $[N_{H_1}, N_{H_2}, N_O]$ depending on two cases of model input for different four ranges of transformation are determined from the minimum of average absolute relative error ($AARE$) as shown in Table 4.1.

Ranges (Li)	Model Input case I (I1)	Model Input case II (I2)
L1=[0.3,0.7]	[24 , 23 , 1]	[17 , 29 , 1]
L2=[0.2,0.8]	[22 , 22 , 1]	[12 , 16 , 1]
L3=[0.1,0.9]	[12 , 12 , 1]	[21 , 16 , 1]
L4=[0.05,0.95]	[19 28 1]	[16 22 1]

Table 4.1: Optimal network structures with two cases of model input (I1 and I2) for each range of the linear transformation (Li).

The statistical comparisons (*AARE, C,* R^2*, NRMSE* and *MDRE*) between the predicted and observed discharges in the testing set with two cases of model input in four ranges of transformation (Li) (see Table 4.1) can be illustrated separately in the Figures 4.1- 4.5.

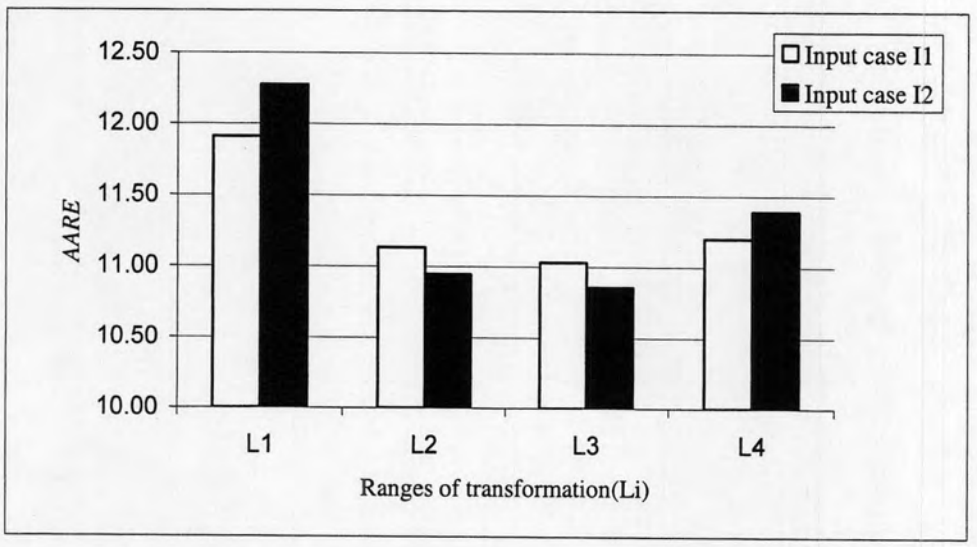

Figure 4.1: Average absolute relative error (*AARE*) of the optimal networks with two cases of model input in four ranges of transformation (Li).

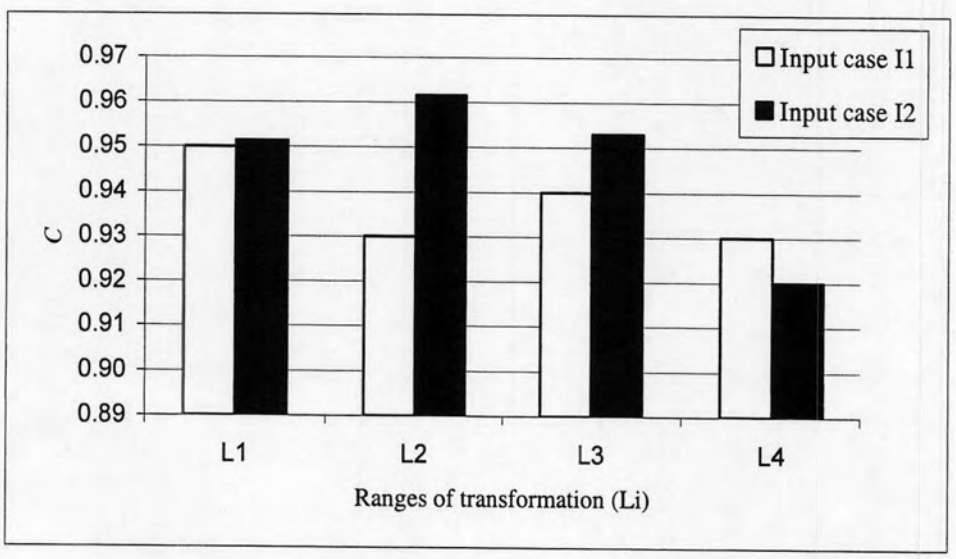

Figure 4.2: Correlation (*C*) of the optimal networks with two cases of model input in four ranges of transformation (Li).

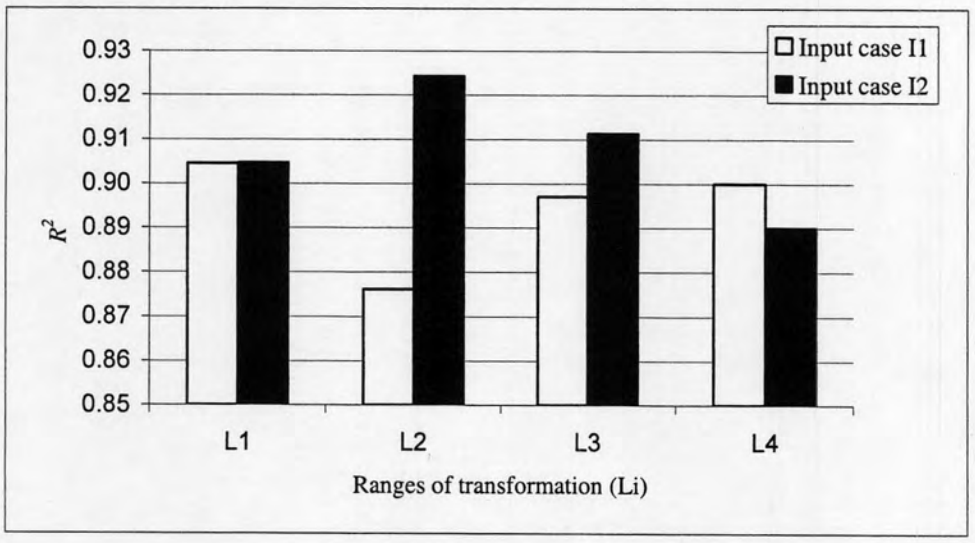

Figure 4.3: Coefficient of determination (R^2) of the optimal networks with two cases of model input in four ranges of transformation (Li).

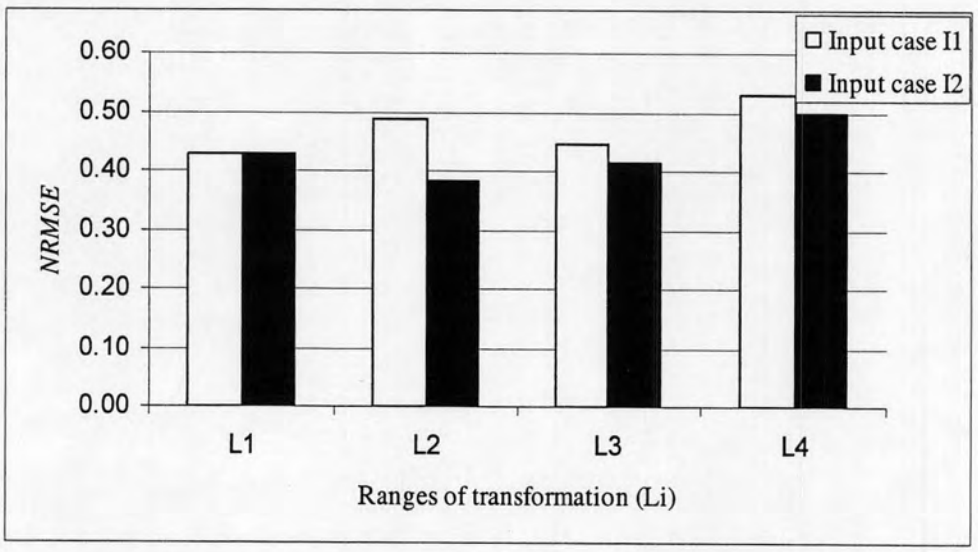

Figure 4.4: Normalized root mean square error (*NRMSE*) of the optimal networks with two cases of model input in four ranges of transformation (Li).

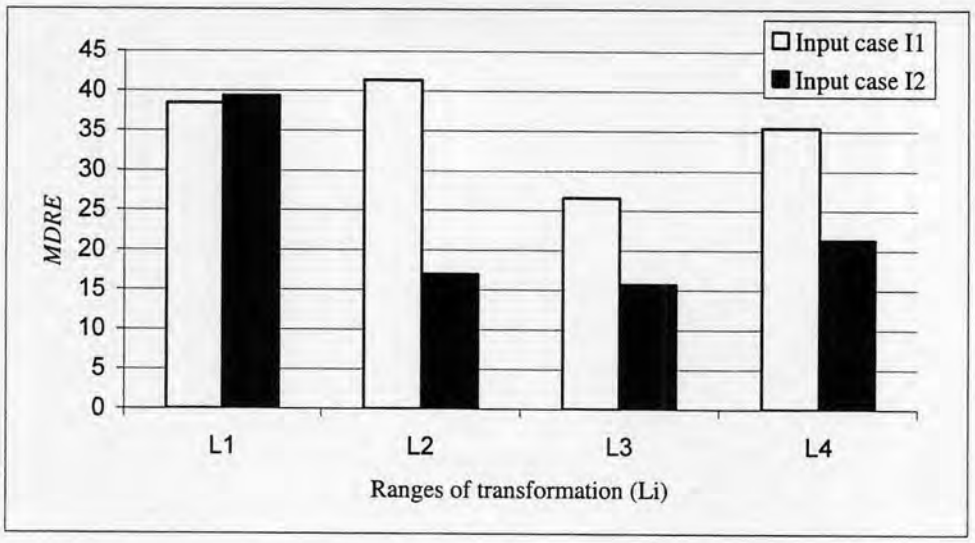

Figure 4.5: Relative error of maximum discharge (*REMD*) of the optimal networks with two cases of model input in four ranges of transformation (Li).

From the above bar charts of five statistics, the model input of case (I1) and (I2) are represented by white and black bars, respectively. Figures 4.1-4.5 show that the model input I2 gives the best statistical value in three ranges of transformation L1, L2 and L3. There is only the *AARE* of range L4 that the model input I1 is better than the model input I2. Although, the *AARE* obtained from model input I1 for range L4 is even less than the *AARE* obtained from model input I2 for ranges L2 and L3. Therefore in this work, the model input of case I2 is selected as the input vector to the network in the studied area. For the selection of the appropriated range of transformation (Li), we will investigate only the case of the model input I2. From Figures 4.1-4.5, it is found that all of five statistic values obtained in the range of L2 and L3 are better than that obtained in the range of L1 and L4. Thus, the suitable range is specifically considered in the range of L2 and L3. From Figures 4.1 and 4.5, both *AARE* and *REMD* values of ranges L2 and L3 with the model input I2 are very close. The C, R^2 and *NRMSE* values (see Figures 4.2, 4.3 and 4.4) of range L2 are, however, better than these values of range L3. Therefore, the ranges L2 ([0.2, 0.8]) is selected as the suitable range of transformation for applying with the model input I2. Finally, we obtain the optimal network of which the structure is [12 16 1] with the model input I2 (4.1) and the range L2 is the used range of linear transformation for input-target pairs.

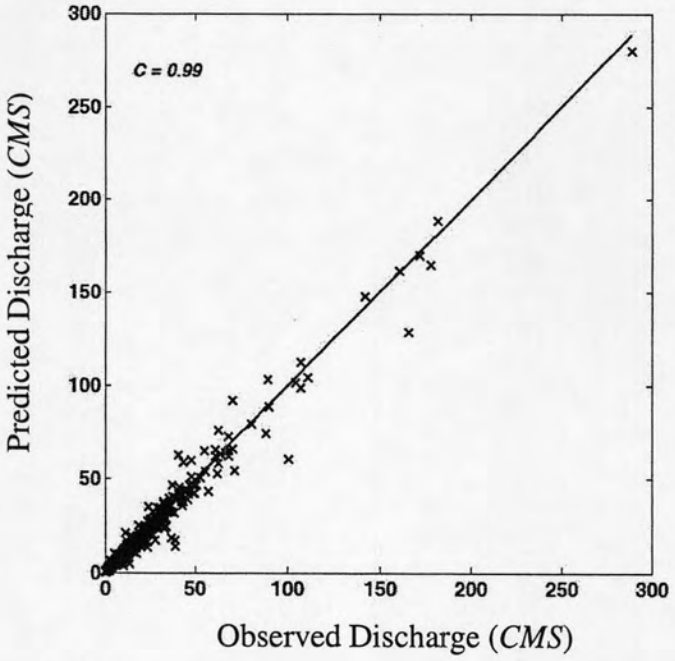

Figure 4.6: Scatter plot of the predicted discharge by ANN model versus the observed discharge for the training set with correlation $C = 0.99$.

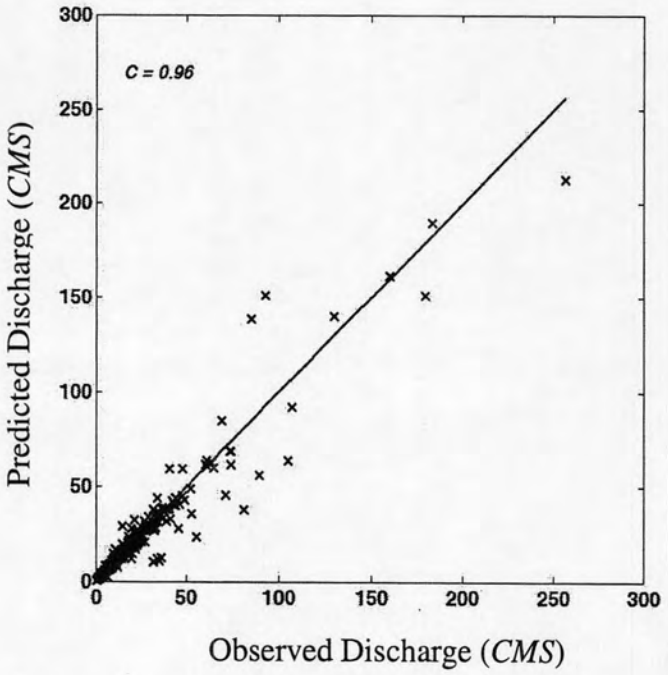

Figure 4.7: Scatter plot of the predicted discharge by ANN model versus the observed discharge for the testing set with correlation $C = 0.96$.

Scatter plots of the predicted discharge by ANN and the observed discharge for the training and the testing sets are shown Figures 4.6 and 4.7, respectively. As illustrated in Fig 4.6, simulation results for the training set show that the constructed network can provide accurate predictions. In case of the testing set, the scatter plot is close to the ideal line. However, there are some values of discharge that the model cannot predict very well. It is resulted from that the rainfall value used in the model input cannot represent the actual distribution of the storm in the watershed.

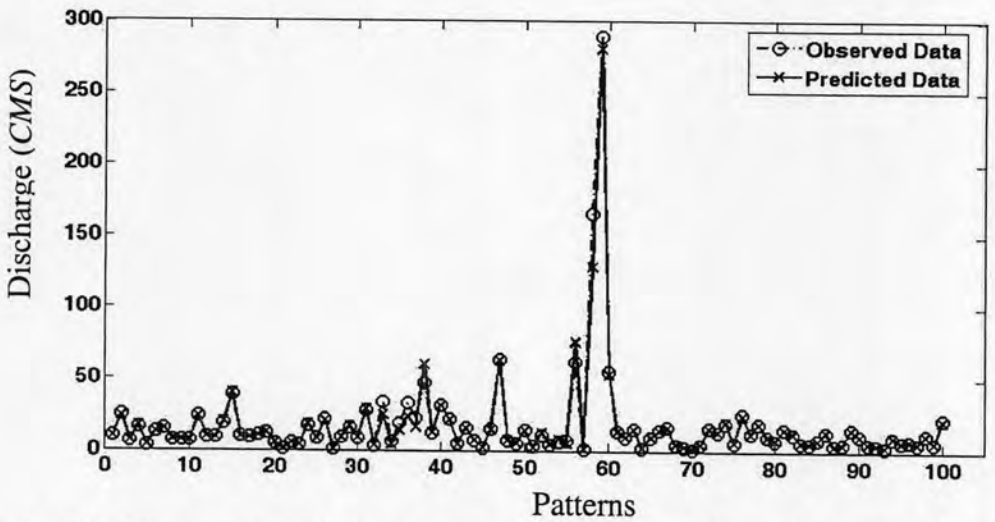

Figure 4.8: Comparison between observed and predicted discharges in the training set.

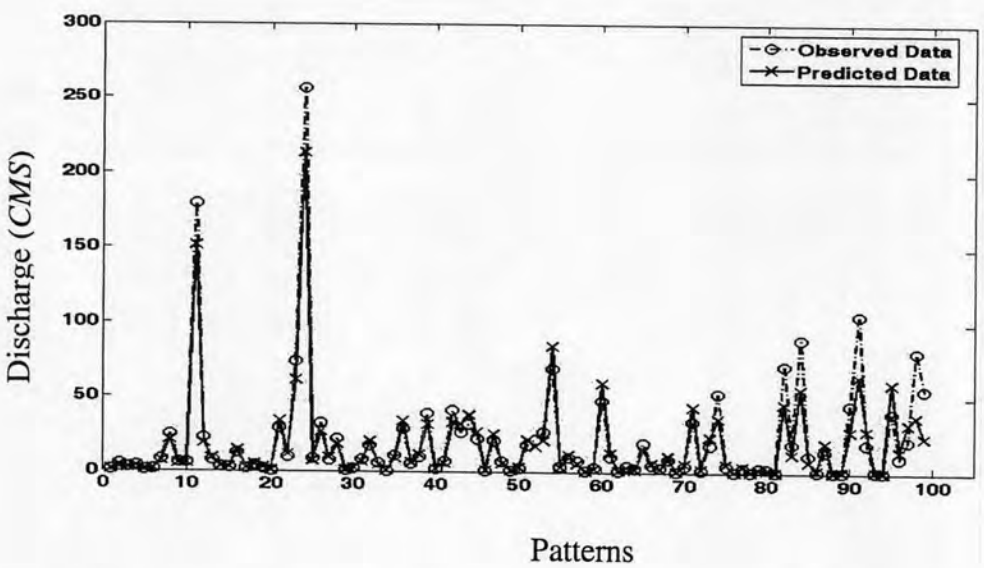

Figure 4.9: Comparison between observed and predicted discharges in the testing set.

Figures 4.8 and 4.9 show the comparison between the observed and predicted discharges for 100 input-target patterns. In the training set, it is found that the predicted discharge from the ANN have good agreement with the observed discharge, especially, the maximum discharge as shown in Figure 4.8. However, from the test results in Figure 4.9, the predicted discharges have good agreement with the observed discharge when the runoff is not too high. There are a few events with high runoff in which ANN suffers some errors in the prediction. This can be explained that, during the storm period, the only rain gauge provides insufficient information for the watershed. However, the overall model performance shows good prediction results especially for the maximum discharge as illustrated in Figure 4.5.

In the same studied area, Pukdeboon (2001) applied Tank model to forecast the three hourly discharges. To compare with the same hydrologic data, 72 patterns of input-target pairs are used for statistical evaluation. The statistics comparison of Tank model and optimal ANN (model input of case I2 with [12 16 1]) are given in Table 4.2.

Model	*AARE*	*C*	R^2	*NRMSE*	*REMD*
Tank	41.35	0.76	0.52	0.60	32.96
ANN	**10.17**	**0.94**	**0.87**	**0.31**	**1.15**

Table 4.2: Statistics comparison of Tank and ANN models with the same hydrologic data for three hourly discharge forecast.

It can be seen from Table 4.2 that all the statistics are consistent. We can be concluded that ANN model outperforms Tank model for forecasting three hourly discharges in the studied area. The scatter plots of the observed discharge versus the predicted discharge by Tank and ANN models with the same hydrologic data are shown in Figures 4.10 and 4.11.

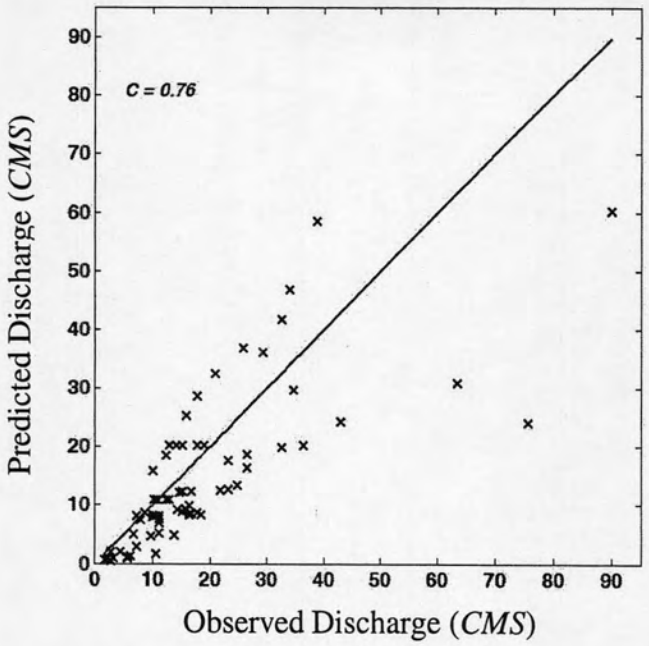

Figure 4.10: Scatter plot of the predicted discharge by Tank model versus the observed discharge with correlation *C=0.76*.

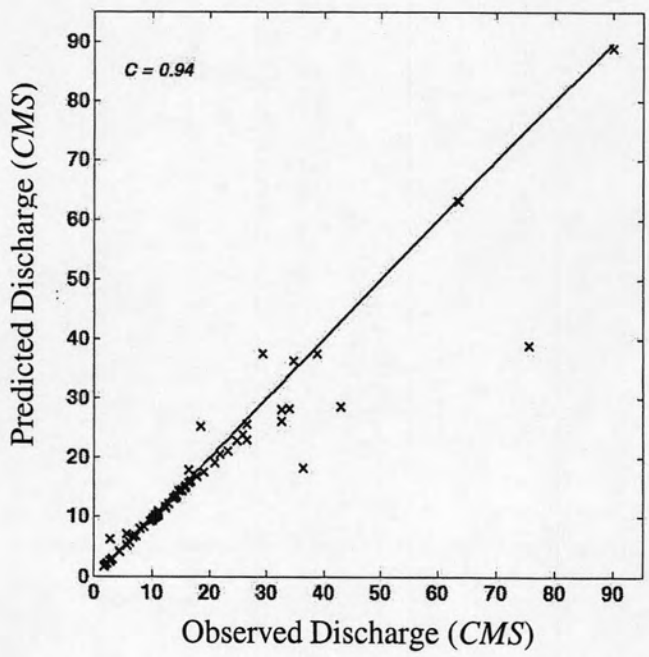

Figure 4.11: Scatter plot of the predicted discharge by ANN model versus the observed discharge with correlation *C=0.94*.

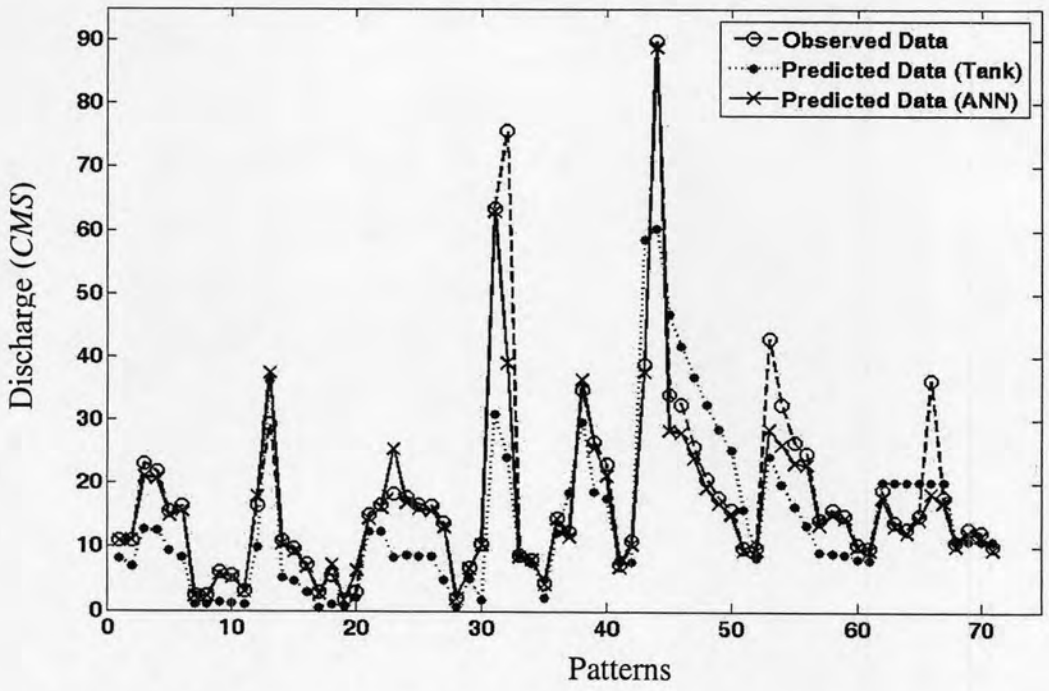

Figure 4.12: Comparison of observed discharge and predicted discharge by Tank and ANN models with the same hydrologic data.

From Figure 4.12, the predicted discharge by ANN fits more properly with the observed discharge than those predicted by Tank model. However, there are some values of discharges that both models cannot accurately predict. This is the case when there has been a rapid increase of the discharge subject to little rainfall intensity for some period of time. Despite of such difficulty, ANN model can still perform better than the Tank model with smaller errors in the predictions.